Journal of Magnetism and Magnetic Materials 330 (2013) 72–75

Contents lists available at SciVerse ScienceDirect

Journal of Magnetism and Magnetic Materials

journal homepage: www.elsevier.com/locate/jmmm

Mössbauer and X-ray diffraction study of Co^{2+}–Si^{4+} substituted M-type barium hexaferrite $BaFe_{12-2x}Co_xSi_xO_{19\pm\gamma}$

E.D. Solovyova [a,*], E.V. Pashkova [a], V.P. Ivanitski [b,1], O.I. V′yunov [a], A.G. Belous [a]

[a] V.I. Vernadskii Institute of General and Inorganic Chemistry, 32/34 Prospect Palladina, Kyiv-142 03680, Ukraine
[b] Institute of Geochemistry, Mineralogy and Ore Formation, 34 Prospect Palladina, Kyiv-164 03680, Ukraine

ARTICLE INFO

Article history:
Received 23 April 2012
Received in revised form
7 September 2012
Available online 30 October 2012

Keywords:
Barium hexaferrite
Non-crystalline material
Precipitation
Mössbauer spectroscopy
Magnetic structure

ABSTRACT

Using X-ray powder diffractions, Mössbauer spectroscopy, and magnetic measurements, the effect of dopants ($Co^{2+}+Si^{4+}$) on the fine structure and magnetic properties of M-type barium hexaferrite prepared by hydroxide and carbonate precipitations has been studied. It has been shown that the magnetic properties of M-type barium hexaferrite can be controlled by heterovalent substitution $2Fe^{3+}\rightarrow Co^{2+}+Si^{4+}$.

1. Introduction

Barium hexaferrite with magnetoplumbite structure M-type BHF is a hard magnetic material. It is characterized by high values of coercivity (H_c) and remanent magnetization (B_r) due to a strong uniaxial magnetocrystalline anisotropy [1,2]. Barium hexaferrite is widely used as a material for new permanent magnets [1–3], high-density data recording and storage systems [4,5], MW devices [6], electromagnetic energy absorbers in the high-frequency range [7–9], or biomedical hyperthermia inductors [10,11]. The requirements for the values of coercivity (H_c) depend on the application of BHF. Characteristic values of coercivity for permanent magnets are 480–640 kA/m and more, for magnetic recording 200–280 kA/m and for biomedical applications as low as possible. The value of the magnetization (M_s) must be high independent of application. Therefore, the preparation of BHF with high M_s and controlled H_c is a problem of today. In recent years, this problem is solved by heterovalent substitution of Fe^{3+} according to the scheme $2Fe^{3+}\rightarrow Me^{2+}+Me^{4+}$, where Me^{2+} and Me^{4+} are ferromagnetic and nonmagnetic ions respectively [12–19]. Such substitution ensures electrical neutrality in the BHF structure. The substitution $2Fe^{3+}\rightarrow Co^{2+}+Ti^{4+}$ is the most studied [12–18]. It is favorable for smooth decrease in H_c with increasing degree of substitution. Depending on the nature of dopants, the magnetization (M_s) of BHF can be unchanged [14], slightly decreased [12], or increased [17].

It is known [1,2,19] that the magnetization of BHF is determined by antiferromagnetic ordering of magnetic ions Fe^{3+}. The distribution of ferromagnetic cations over nonequivalent positions in the M-type BHF structure also affects the magnetization [2,20]. The distribution of cations in ferrites depends on the synthesis conditions and the of dopants nature [1,2,20]. In this work, ($Co^{2+}+Si^{4+}$) ions were chosen as dopants.

It is known that silica (SiO_2) can be used as an inorganic matrix to prepare glass ceramics based on BHF [21,22] and as a material for encapsulating magnetic particles of BHF [23]. However, the effect of substitution of Si^{4+} ions for Fe^{3+} ions is scantily studied [24].

The aim of this work is the investigation of the effect of heterovalent substitution of ($Co^{2+}+Si^{4+}$) ions for Fe^{3+} ions on the crystal structure and magnetic properties of M-type barium hexaferrite.

2. Experimental methods

High purity $Ba(NO_3)_2$, $Fe(NO_3)_3$, $Co(NO_3)_2$ and $(C_2H_5O)_4Si$ were used as initial reagents. The starting hydroxide–carbonate precipitates were obtained by two-step precipitation. The ingredients were precipitated at constant pH. pH was monitored with an I-160 MI ionometer and controlled with a BAT-15 automatic titration unit.

In the first step of precipitation, hydroxides of Fe(III) and Si(IV) were co-precipitated with a water solution of ammonia at pH=4.3. Precipitates were washed in distilled water to remove NH_4^+ ions. In the second step of precipitation, Co(II) and Ba(II) carbonates were co-precipitated with a solution of sodium

* Corresponding author. Tel./fax: +380 44 424 22 11.
E-mail addresses: solovyovak@mail.ru (E.D. Solovyova), pashelena@ukr.net (E.V. Pashkova), vyunov@ionc.kiev.ua (O.I. V′yunov), belous@ionc.kiev.ua (A.G. Belous).
[1] Tel.: +380 44 424 1570; fax: +380 44 424 1211.

0304-8853/$ - see front matter © 2012 Published by Elsevier B.V.
http://dx.doi.org/10.1016/j.jmmm.2012.10.035

carbonate at pH=9. The resulting precipitates were washed free from the mother solution using distilled water until no NO_3^- and Cl^- ions in the washed solution were detected. Powders were dried at 353 K and heat-treated at 1273 K for 2 h.

The samples were characterized by X-ray diffractometry (XRD) using a DRON-3M diffractometer (CuKα radiation, exposure at each point 10 s). SiO_2 (2θ standard) and certified intensity standard Al_2O_3 [25] were used as external standards. For X-ray phase analysis, a JCPDS database was used. The crystal structure parameters were refined by X-ray full-profile analysis.

The size of BHF particle (nm) was estimated from the broadening of the X-ray reflections 110 and 220. BHF calcined at 1773 K for 5 h was used as a standard. The diffraction peak broadening β was calculated from the formula: $\beta=\sqrt{B^2-b^2}$, where B is the total linear broadening of the line, and b is instrumental broadening. The particle size was calculated from the Scherrer formula $D=0.9\lambda/\beta_{hkl}\cos(\theta_{hkl})$[3].

The Mössbauer spectra (MSs) were recorded at room temperature with a spectrometer working in the mode of constant accelerations with the use of ^{57}Co in Cr matrix. The speed scale was calibrated using α-Fe lines. MSs were fitted by the least-square method using Univem-2 software [26].

The magnetic properties of BHF powders were measured in the range of magnetic fields H=0–800 kA/m at room temperature with a ballistic magnetometer.

3. Results and discussion

XRD shows that in the range x=0–0.3 $BaFe_{12-2x}Co_xSi_xO_{19\pm\gamma}$ samples are single-phase ones and have a hexagonal M-type magnetoplumbite structure (space group $P6_3/mmc$). In addition to M-type BHF phase, a $BaFe_{18}O_{27}$ phase with hexagonal W-type structure also appears at $x>0.3$ (Fig. 1). Fig. 2 shows the concentration dependence of the unit cell parameters of M-type BHF. The decrease in V of doped M-type BHF in the homogeneity region (x=0–0.3) on the substitution of $Fe^{3+}_{CN=6,HS}$ ions (r=0.645 Å) [27] by Co^{2+} and Si^{4+} ions (rCo^{2+}_{CN6}=0.735 Å, rSi^{4+}_{CN6}=0.400 Å, $\check{r}$= 0.567 Å) obeys the Vegard rule. This indicates the formation of substitutional solid solutions [28]. The increase in V for $x>0.3$ may be due to increase in the ratio Ba^{2+}/Fe^{3+} content (rBa^{2+}_{CN8}=1.420 Å, rFe^{3+}_{CN6}=0.645 Å) in M-type BHF compared with nominal composition ($1/12-2x$) due to the formation of the second phase, $BaFe_{18}O_{27}$. It is known that solid solution has M-type BHF structure in the range Ba/Fe=1/12−1/8 [29–33].

The concentration dependence of the unit cell parameters of BHF is of a complex character (Fig. 2b) due to the complexity of its crystal structure.

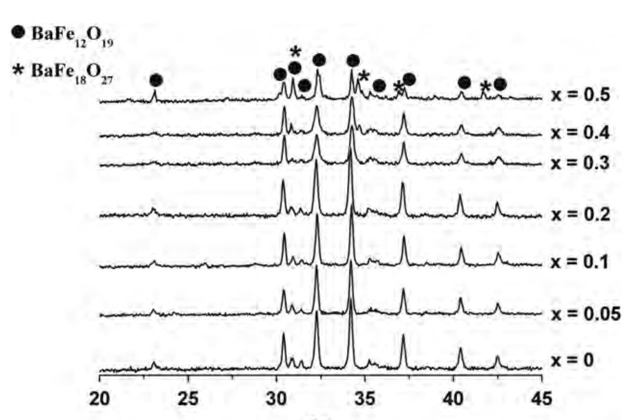

Fig. 1. Diffractograms of $BaFe_{12-2x}Co_xSi_xO_{19\pm\gamma}$ samples calcined at 1273 K.

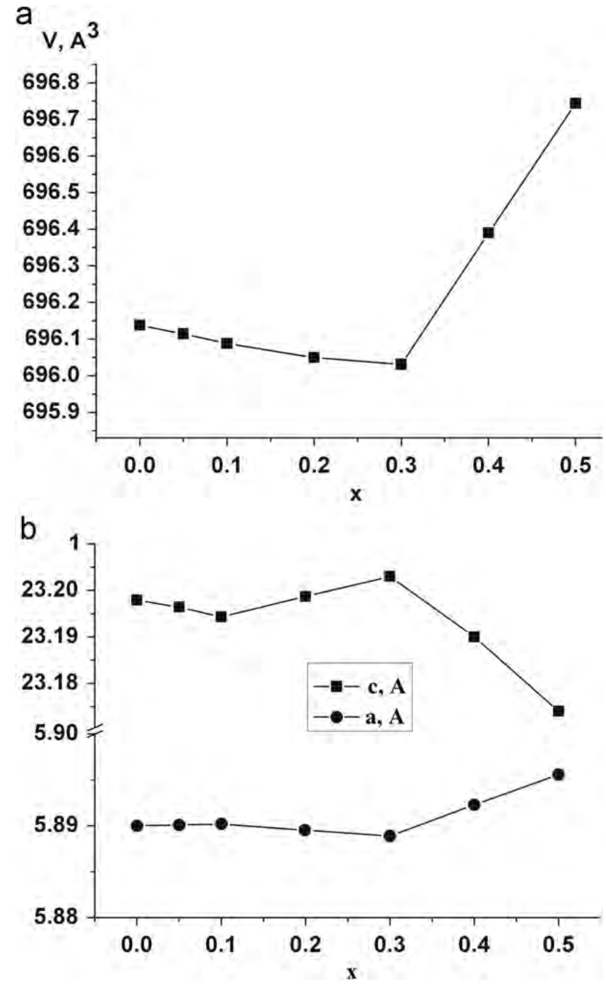

Fig. 2. Concentration dependence of the unit cell volume (a) and parameters (b) of $BaFe_{12-2x}Co_xSi_xO_{19\pm\gamma}$ samples calcined at 1273 K.

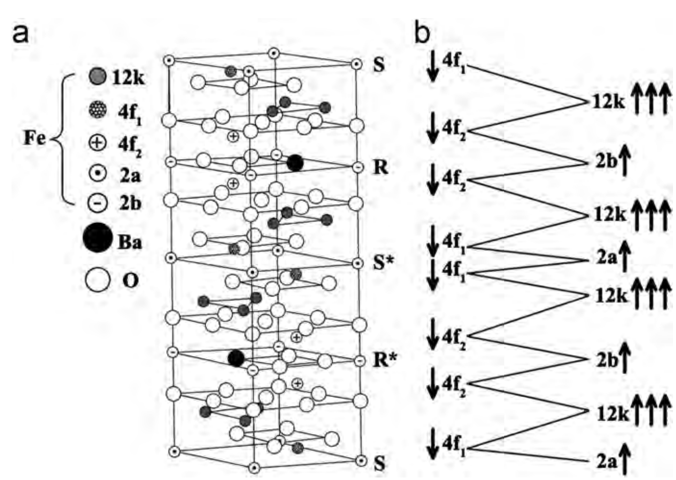

Fig. 3. Crystal (a) and magnetic (b) structures M-type $BaFe_{12}O_{19}$.

Fig. 3 shows crystal and magnetic structures M-type $BaFe_{12}O_{19}$ [34]. The structure of M-type BHF consists of spinel blocks S, S^* and hexagonal barium-containing blocks R, R^*, alternating in the direction of the c axis. S^* and R^* blocks result from rotation of S and R blocks by 180° about the c axis. The unit cell of BHF contains 10 layers of O^{2-} ions (Fig. 3). There are five

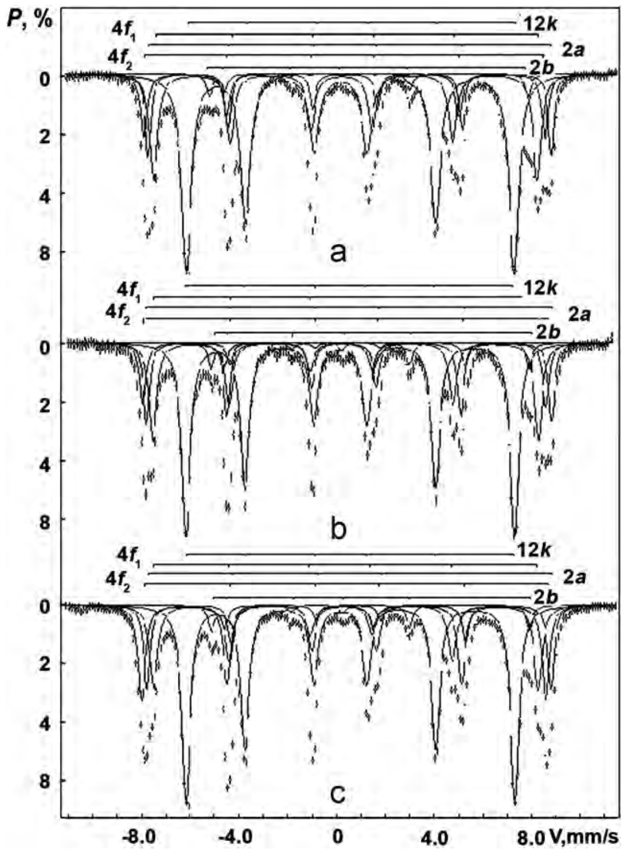

Fig. 4. Mössbauer spectra of $BaFe_{12-2x}Co_xSi_xO_{19\pm\gamma}$ samples calcined at 1273 K: $x=0$ (a); 0.1 (b); and 0.3 (c).

nonequivalent crystallographic positions of iron ions in the structure. Three positions are octahedral (12*k*, 4f_2 and 2*a*), one is tetrahedral (4f_1), and one is inside oxygen bipyramid (2*b*).

MSs of $BaFe_{12-2x}Co_xSi_xO_{19\pm\gamma}$ samples are shown in Fig. 4, and their parameters are listed in Table 1. The MS lines were assigned to structural positions by the model described in Refs. [35–38]. According to this model, each of the five iron positions in the BHF structure produces a resonance sextet of magnetic interaction. This model allows one to estimate the occupation of structural positions by Fe^{3+} ions. The parameters of MSs correspond to the high-spin Fe^{3+} ions in octahedral (12*k*, 4f_2 and 2*a*), tetrahedral (4f_1) and bipyramidal (2*b*) coordinations of M-type BHF [17,35–38]. For calculation, various software and approaches were used [39]. We assumed that widths of the lines in the sextets are the same, and the ratio of line intensities of sextets is 3:2:1:1:2: 3. The change of the software and calculation method does not affect significantly the MS parameters and the concentration dependence of occupation Fe^{3+} ions position. If the positions are uniformly occupied and the resonance absorption coefficients are equal, then the ratio of the sextet areas relating to the iron positions 12*k*:4f_2:4f_1:2*b*:2*a* must be 50:17:17:8:8. The difference between experimental and theoretical occupancies may be associated with a significant influence of BHF synthesis conditions on the distribution of Fe^{3+} ions over positions.

Fig. 5 shows the dependence of the relative areas of sextets on the degree of substitution of Fe^{3+} ions in the homogeneity region of $BaFe_{12-2x}Co_xSi_xO_{19\pm\gamma}$ (x=0–0.3). This dependence correlates with the concentration dependence of unit cell parameters (Fig. 2b). The areas of the MS sextets corresponding to the 12*k* and 2*a* positions of BHF ($x=0$) coincide with the theoretical values (within experimental errors) (Table 1 and Fig. 5). The areas of the 4f_1 sextets are larger and those of 4f_2, 2*b* and 2*a* are

Table 1
Parameters of Mössbauer spectra of barium hexaferrites $BaFe_{12-2x}Co_xSi_xO_{19\pm\gamma}$.

No.	Parameters	Sample	Ion (position)				
			Fe^{3+}(12*k*)	Fe^{3+}(4f_1)	Fe^{3+}(4f_2)	Fe^{3+}(2*a*)	Fe^{3+}(2*b*)
1	H_{eff} (kOe)	$x=0$	416	487	512	509	404
		$x=0.1$	417	489	514	511	403
		$x=0.3$	417	487	513	513	403
2	IS (mm/s)	$x=0$	0.37	0.29	0.45	0.30	0.28
		$x=0.1$	0.35	0.28	0.47	0.30	0.29
		$x=0.3$	0.37	0.29	0.50	0.31	0.30
3	QS (mm/s)	$x=0$	0.40	0.16	0.18	0.07	2.12
		$x=0.1$	0.41	0.19	0.07	0.02	2.18
		$x=0.3$	0.41	0.21	0.02	0.02	2.19
4	*W* (mm/s)	$x=0$	0.47	0.39	0.26	0.31	0.28
		$x=0.1$	0.41	0.36	0.29	0.31	0.27
		$x=0.3$	0.41	0.38	0.30	0.34	0.29
5	*S* (%)	$x=0$	52.4	23.4	12.1	9.1	3.0
	(*C*(Fe^{3+}))		(12.6)	(5.6)	(2.9)	(2.2)	(0.7)
		$x=0.1$	50.0	19.8	9.5	16.2	4.5
			(11.8)	(4.7)	(2.2)	(3.8)	(1.1)
		$x=0.3$	46.1	17.6	11.5	20.4	4.4
			(10.5)	(4.0)	(2.6)	(4.7)	(1.0)

Note: *Heff*magnetic field, kOe.
IS=isomer shift relative to metallic iron, mm/s.
QS=quadrupole splitting, mm/s.
W=absorption line half-width, mm/s.
S=relative component area, %.
Measurement error: H_{eff}—5 kA/m; IS, QS; *W*—0.04 mm/s; *S*—6%.

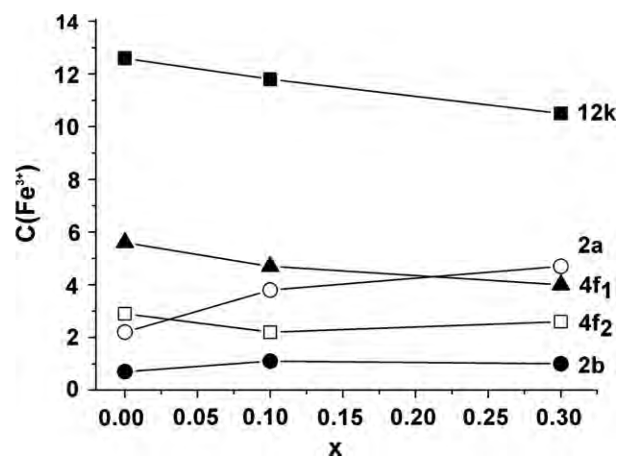

Fig. 5. Dependences of Fe^{3+} ions concentration on *x* at the positions 12*k*, 4f_2, 4f_1, 2*b* and 2*a* of $BaFe_{12-2x}Co_xSi_xO_{19\pm\gamma}$.

smaller than the theoretical values. The same results have been obtained by us for $BaFe_{12-2x}Co_xTi_xO_{19\pm\gamma}$ [17].

It is known that Fe^{3+} ions have a spherically symmetric $3d^5$ electronic shell. Therefore, Fe^{3+} ions are distributed uniformly over the tetra- and octahedral positions of spinel structure [20]. The Fe^{3+} ions in BHF ($x=0$) prefer to occupy tetrahedral 4f_1 positions in the spinel blocks *S* and *S** (see Fig. 3). Fig. 5 and Table 1 show that in the range $0.1<x\leq 0.3$ the areas of the components 12*k* and 4f_1 decrease, but that of 4f_2 increases on the substitution $2Fe^{3+}\rightarrow Co^{2+}+Si^{4+}$. The decrease in the areas of MS components indicates that the concentration of Fe^{3+} ions in this positions and the occupation of Si^{4+}, Co^{2+} ions decrease.

It is known that the formation of four equivalent hybrid sp^3-orbitals is characteristic of silicon in compounds [40]. Therefore Si^{4+} ions prefer tetrahedral coordinations 4f_1. Whereas Si^{4+} ions occupy 4f_1 position, Fe^{3+} ions in the ranges $0<x<0.1$ and $0.1\leq x\leq 0.3$ prefer octahedral positions 2*b*, 2*a* and 4f_2, 2*a*

Table 2
Magnetic properties and particle size of $BaFe_{12-2x}Co_xSi_xO_{19\pm\gamma}$ samples calcined at 1273 K.

Sample	d (nm)	M_s (Am^2/kg)	M_r (Am^2/kg)	M_r/M_s	H_c (kA/m)
$x=0$	71	43.7	22	0.5	280
$x=0.1$	38	49.5	27	0.55	104
$x=0.3$	42	60.1	32	0.53	96

respectively (Fig. 5). Co^{2+} ions prefer octahedral coordination due to d^2sp^3 hybridization and can occupy 12k position [1,20,41].

As shown in Table 1, parameters H_{eff}, IS and W do not change with increasing degree of substitution (x). This indicates that the electronic configuration of Fe^{3+} ions remains unchanged on the substitution $2Fe^{3+} \rightarrow Co^{2+} + Si^{4+}$. Dynamics of change in quadrupole splitting (QS) with increasing x is observed for positions $4f_1$, $2b$, $4f_2$ and $2a$ (QS increases for positions $4f_1$ and $2b$, and decreases for positions $4f_2$ and $2a$). The increase of QS for $4f_1$ sextet may be associated with a distortion of the oxygen tetrahedron due to the substitution of Si^{4+} ions for Fe^{3+} ions. Anomalously large values of QS for Fe^{3+} ($2b$) sextet are probably due to the strong symmetry breaking of bipyramidal anionic environment. The presence of anisotropy of the mean-square shift of Fe^{3+} ion along the c axis in position $2b$ confirms this [35]. QS increases for $2b$ sextet with increasing Fe^{3+} ion concentration and degree of substitution (Table 1, Fig. 5).

The particle size of BHF decreases due to the substitution of Co^{2+} and Si^{4+} ions for Fe^{3+} ions (Table 2). The coercivity (H_c) of $BaFe_{12-2x}Co_xSi_xO_{19\pm\gamma}$ samples decreases with increasing x and is 378, 104 and 96 kA/m for $x=0$, 0.1 and 0.3 respectively (Table 2). The decrease in H_c may be attributed to a decrease in the magnetocrystalline anisotropy constant (K) of $BaFe_{12-2x}Co_xSi_xO_{19\pm\gamma}$ samples as compared to $BaFe_{12}O_{19\pm\gamma}$ samples [1]. It should be noted that for the control of coercivity (H_c), a combination of $Co^{2+}+Si^{4+}$ ions is more effective than that of $Co^{2+}+Ti^{4+}$ ions [17].

The magnetization (M_s) of samples with $x=0$, 0.1, 0.3 increases with x and is 43.7, 49.5 and 60.1 kA/m^2, respectively.

The magnetic moment of BHF sample is determined as the algebraic sum of magnetic moments of ions in different positions:$M_s = M_s(\overrightarrow{12k}+\overrightarrow{2b}+\overrightarrow{2a}) - M_s(\overleftarrow{4f_2}+\overleftarrow{4f_1})$ (Fig. 3b) [2]. It is evident that the increase in the magnetization of modified BHF (Table 2) results from an increase in the concentration of ferromagnetic ions (Fe^{3+} and Co^{2+}) in the positive component $M_s = M_s(\overrightarrow{12k}+\overrightarrow{2b}+\overrightarrow{2a})$and a decrease in Fe^{3+} ion concentration in the negative component $M_s = M_s(\overleftarrow{4f_2}+\overleftarrow{4f_1})$ (Fig. 5, Table 1).

4. Conclusion

The effect of ($Co^{2+}+Si^{4+}$) dopants on the fine structure and magnetic properties of M-type BHF has been studied.

It has been found that in the range $x=0$–0.3, homogeneous substitutional solid solutions $BaFe_{12-2x}Co_xSi_xO_{19\pm\gamma}$ are formed.

The presence of only Fe^{3+}ions in the high-spin state in the homogeneous region has been detected.

It has been shown that in M-type barium hexaferrites Ba $Fe_{12-2x}Co_xSi_xO_{19\pm\gamma}$, Co^{2+} and Si^{4+} ions prefer to occupy crystallographic positions $12k$ and $4f_1$ respectively. Si^{4+} prefers to occupy tetrahedral positions $4f_1$ and Co^{2+} ion prefers to occupy octahedral positions $12k$.

It has been shown that substitution $2Fe^{3+} \rightarrow Co^{2+} + Si^{4+}$ contributes to decrease in particle size and coercivity (H_c) and increase in the magnetization (M_s) of BHF.

References

[1] S. Krupichka, Physics of Ferrites and Allied Magnetic Oxides, Mir, Moscow, 1976.
[2] J. Smith, H.P.J. Wijn, Ferrites, Philips Technical Laboratory, Eindhoven, 1961.
[3] S.P. Gubin, Yu A. Koksharov, G.B. Khomutov, G.Yu Yurkov, Russian Chemical Reviews 74 (2005) 489–524.
[4] F. Lei, L. Xiaogang, Y. Zhang, P.D. Vinayak, A.M. Chad, Nano Letters 3 (2003) 757–760.
[5] Q.A. Pankhurst, R.S. Pollard, Journal of Physics: Condensed Matter 5 (1993) 8487–8508.
[6] S.V. Lebedev, C.E. Patton, M.A. Wittenauer, L.V. Saraf, R. Ramesh, Journal of Applied Physics 91 (2002) 4426–4431.
[7] Z. Haijun, L. Zhichao, Ma Chenliang, Y. Xi, Z. Liangying, Materials Science and Engineering B 96 (2002) 289–295.
[8] T. Kagotani, D. Fujiwara, S. Sugimoto, K. Inomata, M.J. Homma, Journal of Magnetism and Magnetic Materials 2004 (1813) 272–276.
[9] M.R. Meshram, N.K. Agarwal, B. Sinha, P.S. Misra, Journal of Magnetism and Magnetic Materials 271 (2004) 207–214.
[10] R. Muller, R. Hergt, S. Dutz, M. Zeisberger, W. Gawalek, Journal of Physics: Condensed Matter 18 (2006) 2527–2542.
[11] E. Pollert, P. Veverka, M. Veverka, O. Kaman, K. Zaveta, S. Vasseur, R. Epherre, G. Goglio, E. Duguet, Progress in Solid State Chemistry (2009) 1–14.
[12] H.Y. He, J.F. Huang, L.Y. Cao, J.P. Wu, Q. Shen, Materials Technology 2 (2007) 30–32.
[13] N. Koga, T. Tsutaoka, Journal of Magnetism and Magnetic Materials 313 (2007) 168–175.
[14] Z. Haijun, L. Zhichao, Ma Chenliang, Y. Xi, Z. Liangying, W. Mingzhong, Materials Chemistry and Physics 80 (2003) 129–134.
[15] G. Mendoza-Suareza, J.C. Corral-Huacuz, M.E. Contreras-Garcia, H. Juarez-Medinab, Journal of Magnetism and Magnetic Materials 234 (2001) 73–79.
[16] D. Lisjak, M. Drofenik, Journal of the European Ceramic Society 24 (2004) 1841–1845.
[17] A.G. Belous, O.I. Vyunov, E.V. Pashkova, V.P. Ivanitskii, O.N. Gavrilenko, Physical Chemistry B 110 (2006) 26477–26481.
[18] S.Y. An, S.W. Lee, I.B. Shim, C.S. Kim, Journal of Applied Physics 91 (2002) 8465–8467.
[19] X. Tang, Y. Yuanguang, K. Hu, Journal of Alloys and Compounds 477 (2009) 488–492.
[20] B.Ye Levin, Yu D. Tretyakov, L.M. Letyuk, Physicochemical Fundamentals of the Preparation of Ferrites, Their Properties and Applications, Metallurgiya, Moscow, 1979.
[21] I.H. Araujo, F.A.O. Cabral, M.E. Ginai, J.M. Soares, F.L.A. Machado, Journal of Non-Crystalline Solids 352 (2006) 3518–3521.
[22] S. Ponce-Castaneda, I.R. Martinez, F. Ruiz, S. Palomares-Sanchez, Journal of Magnetism and Magnetic Materials 250 (2002) 160–163.
[23] W. Fu, H. Yang, Q. Yu, J. Xu, X. Pang, G. Zou, Materials Letters 61 (2007) 2187–2190.
[24] S.M. Abbas, R. Chatterjee, A.K. Doxit, A.V.R. Kumar, T.C. Goel, Journal of Applied Physics 101 (2007) 074105.
[25] S. Rosler, P. Wartewing, H. Laugbein, Crystal Research and Technology 38 (2003) 927–934.
[26] Univem-Ms Version Beta Program Manual, Scientific Research Institute of Physics, Rostov-Na-Donu State University, 2001, (in Russian).
[27] R.D. Shanon, Acta Crystallographica 32 A (1976) 751–767.
[28] A.R. West, Solid State Chemistry and its Application, Wiley, New York, 1984.
[29] M.M. Rashad, M. Radwan, M.M. Hessien, Journal of Alloys and Compounds 453 (2008) 304–308.
[30] M. Mozaffari, M. Taheri, J. Amighian, Journal of Magnetism and Magnetic Materials 321 (2009) 1285–1289.
[31] S. Salemizadeh, S.A. Seyyed Ebrahimi, Journal of Non-Crystalline Solids 355 (2009) 982–985.
[32] L. Hai-Feng, G. Rong-Zhou, L. Xiu-Fang, L. Xiu-Fang, Y. Wei, W. Xian, F. Li-Ren, H. Gang, Journal of Inorganic Chemistry 26 (2011) 792–796.
[33] G. Mendoza-Suarez, J.A. Matutes-Aquino, J.I. Escalante-Garcia, et al., Journal of Magnetism and Magnetic Materials 223 (2001) 55–62.
[34] C.S. Kim, S.W. Lee, S.Y.J. An, Journal of Applied Physics 87 (2000) 6244–6246.
[35] B.I. Evans, F. Grandjean, A.P. Lilot, Journal of Magnetism and Magnetic Materials 67 (1987) 123–129.
[36] G.K. Thompson, B.I. Ebans, Journal of Magnetism and Magnetic Materials 95 (1991) L142–L144.
[37] F. Leccabue, R. Panizzieri, S. Garsia, Journal of Materials Science 25 (1990) 2765–2770.
[38] X. Obradors, X. Solands, A. Collomb, Journal of Solid State Chemistry 72 (1988) 218–224.
[39] A.A. Novakova, T.Yu Kiseleva, Mössbauer Practical Work (Rus), Moscow, Moscow State University, 2000.
[40] V.S. Gorshkov, V.G. Savelev, N.F. Fedorov, Physical Chemistry of Silicates and Other Hardly Fusible Compounds, Vysshaya Shkola, Moscow, 1988.
[41] L.E. Orgel, An Introduction to Transition-Metal Chemistry, Wiley, New York, 1960.